All-d-Metal Heusler Alloys

Subjects: Chemistry, Inorganic & Nuclear | Physics, Applied
Contributor: Tarek Bachagha, Joan-Josep Suñol

A promising strategy, resulting in novel compounds with better mechanical properties and substantial magnetocaloric effects, is favoring the *d*–*d* hybridization with transition-metal elements to replace *p*–*d* hybridization. The term given to these materials is “all-*d*-metal”.

Keywords: Heusler alloys ; hybridization ; magnetocaloric effect

1. Background of These Kinds of Alloys

Recently, Wei et al. [1] suggested the notion of an all-*d*-metal Heusler based on *d*–*d* orbital hybridization. The authors of this seminal work established the term “all-*d*-metal” after discovering that the Heusler phase could be formed without the *p*-group atom. Experiments on the crystal structure of Zn_2AuAg and Zn_2CuAg compounds [2][3] may be traced all the way back to the 1960s. Both compounds have $L2_1$ organized and *B2* disordered structures, according to these ancient publications. The Zn_2AuAg, in particular, shows a *B2* to $L2_1$ order-disorder transition, as evidenced by changes in structural order characteristics. On the other hand, their applications as FSMAs are limited due to the absence of FM ordering in these alloys, and no further research on these alloys has been conducted. Both alloys now belong within the category of Heusler alloys since the notion of all-*d*-metal Heusler is widely known.

2. Crystalline Structure

In the recently found $Ni_2Mn_{2-y}Ti_y$ and $Ni_{2-y}Mn_2Ti_y$ systems, Ti atoms have the fewest valence electrons ($3d^24s^2$) compared to Ni ($3d^84s^2$) and Mn ($3d^54s^2$), and Wei et al. [1] predicted that Ti would occupy the D site. Both systems crystallize in a *B2*-type disordered structure, with the Mn excess atoms sharing the D site with Ti atoms in the $Ni_2Mn_{2-y}Ti_y$ system, resulting in a strong AFM coupling due to the Mn(B)–Mn(D) interaction (**Figure 1**). The main difference with conventional Heusler alloys is the competence between the $L2_1$ and the inverse *XA* phases.

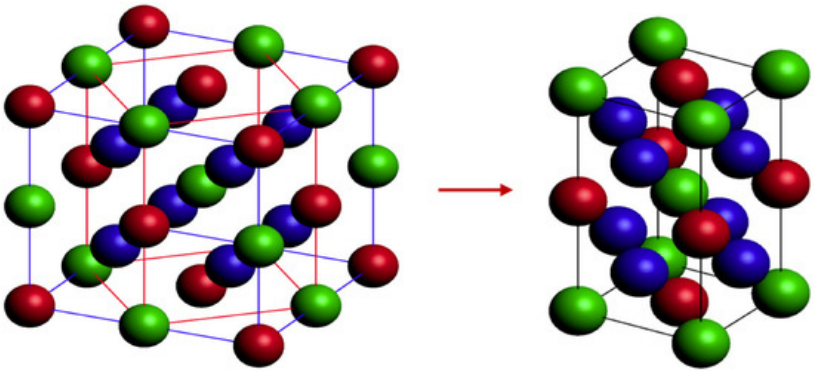

Figure 1. Schema of the $L2_1$ Heusler crystallographic structure (**left**) indicating with red lines the cell of the $L1_0$ tetragonal martensite (**right**) for stoichiometric $Ni_{50}Mn_{25}Ti_{25}$ alloy.

The $Ni_{2-x}Co_xMn_{1.4}Ti_{0.6}$ quaternary series was discovered by Wei et al. [4], who employed the strategy of introducing Co atoms at Ni sites to impose FM long-range ordering on the Ni–Mn–Ti system, resulting in the first FSMAs among all-*d*-metal Heusler alloys. Partially replacing Co atoms in Ni_2MnZ systems has previously been investigated [5], resulting in a strong local Mn(B)–Co(A/C)–Mn(D) exchange coupling with FM ordering [6], overcoming the Mn(B)–Mn(D) AFM coupling inherent in the *B2*-type disordered lattice. Moreover, some experimental results observed that strong ferromagnetism provides direct evidence of this probable atomic configuration and of the ferromagnetic activation effect in the Ni(Co,Fe)–Mn–Ti all-*d*-metal Heusler alloys. For example, in $Ni_{50-x}Co_xMn_{35}Ti_{15}$ alloys, Co atoms that have been substituted for Ni atoms will also share the (A,C) sites with Ni atoms, leaving Mn and Ti with fewer valence electrons at the B/D sites. With the aid of the strong FM exchange interactions between nearest-neighbor Co-Mn atoms, the original AFM exchange

coupling between Mn-Mn atoms in Ni-Mn-Ti alloys is converted into FM one, resulting in parallel alignment of the Mn-Co-Mn moments [4]. This phenomenon is known as the “ferromagnetic activation effect of the Co atom” [6]. FM ordering in $Ni_{2-x}Fe_xMn_{1.4}Ti_{0.6}$ alloys [7], in which Fe substitutes Co in the exchange coupling, is generated via a similar mechanism. Co ($3d^74s^2$) and Fe ($3d^64s^2$) atoms are considered to share the (A/C) sites with Ni ($3d^84s^2$) atoms in both series since their valence numbers are greater than those of Mn and Ti. Feng [8] used theoretical calculations on the X_2MnTi (X = Pt and Pd) series to study the impact of Ti as a *p*-group atom replacement. The findings show that the $L2_1$ crystallographic structure is energetically stable for both compositions, with high valence Pd ($4d^85s^2$) and Pt ($5d^86s^2$) filling the (A/C) sites and Mn ($3d^54s^2$) occupy the (B) site, respectively. Ti prefers to remain in the D site. Han et al. [9] developed research for all-*d*-metal Heusler alloys $X_{2-x}Mn_{1+x}V$ (X = Pd, Ni, Pt, Ag, Au, Ir, Co; x = 1, 0). They looked at the atomic occupancy of these alloys in the cubic phase and discovered that the well-known site preference criterion does not apply to all of them. Han et al. [10][11] and Wang et al. [12] studied other Zinc-based all-*d*-metal Heusler ZnCdTMn combinations by theoretical calculations on the Zn_2YMn series. As a result of its complete 3*d* occupied state, the Zn atoms behave as a major group element, and Zn atoms prefer to occupy the D site rather than replacing Pd atoms at site A. The phenomenon of this process is the whole 3*d* shell of the Zn atom.

In **Figure 1**, as the content of Ti was usually lower than 25 at.%, some Mn atoms are located on D sites by substituting Ti atoms. However, the martensitic crystallographic structure can be more complex, including modulation, as shown in **Figure 2**.

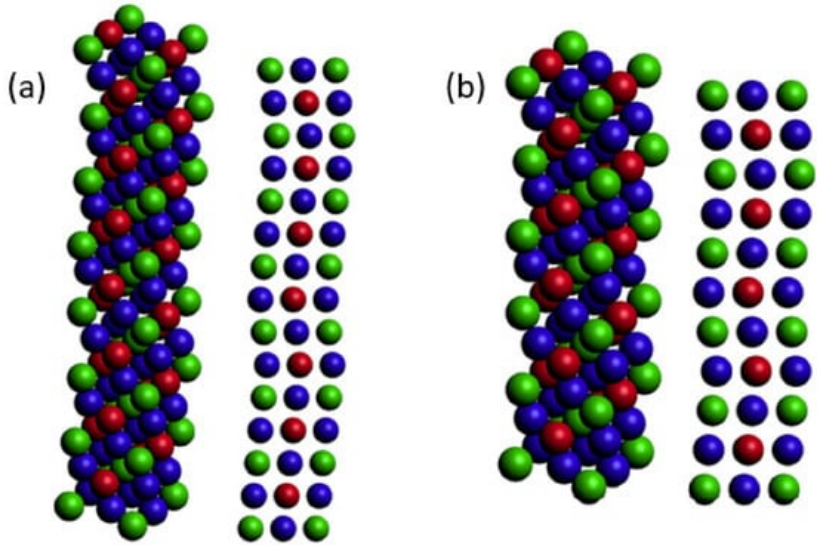

Figure 2. (**a**) Cell of the seven-layer modulated martensite phase (14M) of an arbitrary composition sample seen in 3D and laterally. (**b**) Cell of the five-layer modulated martensite phase (10M) of an arbitrary composition sample seen in 3D and laterally (generated with MAUD-free software, version 2.08, Luca Lutterotti, Trento, Italy).

3. Influence of d–d Hybridization

Theoretical calculations revealed that stoichiometric Ni_2MnTi displays mechanical properties superior to those of conventional Heusler systems. Yan et al. [13] later discovered that the $Ni_{2.0}Mn_{1.27}Ti_{0.73}$ composition has a significant eCE (under 600 MPa of uniaxial stress, adiabatic temperature change ΔT_{ad} = −20.4 K). Many Ni–Mn-based systems, such as $Ni_{1.80}Mn_{1.76}Sn_{0.44}$ (ΔT_{ad} = −11.6 K unloading 600 MPa of uniaxial stress) [14] and $Ni_{2.0}Mn_{1.11}Ga_{0.89}$ (unloading 100 MPa of uniaxial stress, ΔT_{ad} = −6.1 K) [15], have lower values. Changing the chemical bonding character of the $Ni_{2.0}Mn_{1.27}Ti_{0.73}$ all-*d*-metal Heusler alloy by substituting high *p*–*d* hybridization with somewhat weaker *d*–*d* hybridization among transition metals increases its ductility, according to further examination of the electron localization function. Pugh’s ratio [16] is a popular metric for determining solid ductility. It is defined as the ratio of the bulk modulus B to the shear modulus G of a material. Values greater than 1.75 indicate ductile behavior. Researchers see that Ni_2MnTi is more ductile than Ni_2MnGa [17] and Ni_2MnIn [18], two of the most promising FSMAs among Heusler systems, according to the results. Furthermore, Ni_2MnTi [19] also has the highest Cauchy pressure, indicating that chemical bandings are weakly covalent. As a consequence, reducing covalent *p*–*d* hybridization in Ni_2MnZ Heusler alloys is connected to enhanced ductility.

4. MCE in All-d-Metal Heusler Alloys

Until recently, only a few investigations have focused on Heusler alloys of this type. Wei et al. [1] recently discussed the creation of all-*d*-metal alloys that exclusively include 3*d* transition metal components. They found that adding Ti to Ni–Mn

aids in the *B2* phase creation and stability. Cong et al. [20] achieved a massive elastocaloric impact in Ni–Mn–Ti alloys, with a ΔT_{ad} = 31.5 K and ΔS_M = 45 $Jkg^{-1}K^{-1}$, at a pressure of 700 MPa. Yan et al. [11] also discovered that the bulk $Ni_{50}Mn_{31.75}Ti_{18.25}$ alloy has outstanding mechanical characteristics, with a stress of 1.1 GPa and a convincing compressive strain of 13%, respectively. Despite its exceptional elastocaloric sway, the Ni–Mn–Ti combination has a modest MCE when compared to Heusler alloys. The absence of magnetic contrast between the austenite and martensite phases is largely responsible for this. Yan et al. [13] examined the austenite phase's antiferromagnetic condition in Ni–Mn–Ti alloys. As a result, some thought has been given to doping the elements to improve the magnetocaloric impact. Furthermore, according to Wei et al. [4], cobalt doping in the $Ni_{50}Mn_{35}Ti_{15}$ alloy affects the transition from AFM to FM in the austenite phase. They created the Mn–Co–Mn configuration by replacing Co for Ni sites in the austenite phase, resulting in the ferromagnetic activation effect. Additionally, the AFM state of austenite in Ni–Mn–Ti alloys was confirmed by Yan et al. [13] and Wei et al. [4]. Therefore, some researchers have attempted to improve its MCE by means of doping elements. Li et al. [21] indicated that under a magnetic field of 3 T, Fe and Co doping in the Ni–Mn–Ti alloy could produce the refrigeration capacity (RC) of 79.5 Jkg^{-1} and ΔS_M of 8.4 $Jkg^{-1}K^{-1}$. In addition, taking into account the magnetostructural coupling in the $Ni_{2-x}Fe_xMnTi$ [15] and Ni–Co–Mn–Ti [7] Heusler alloys, a giant MCE was observed. Recently, Aznar et al. [22][23] revealed the B-doped $Ni_{50}Mn_{31.5}Ti_{18.5}$ all-*d*-metal Heusler alloy. These alloys created an excellent BCE with an RC up to 1100 Jkg^{-1} and ΔS_M of 74 $Jkg^{-1}K^{-1}$ under the pressure of 3.8 kbar, undergoing MT with an enormous volume change (ΔV) in its PM. Due to the eCE and MCE coexisting near RT, these alloys must be candidates for magnetic refrigeration.

5. Perspectives

Recently, experimental efforts targeted at increasing the MCE of all-*d*-metal Heusler alloys are worth emphasizing. One option is to add more elements to analyze multicomponent specimens and the effect of the combination of four or fifth elements in the functional response in a similar pathway to the applied to conventional Heusler alloys. Taubel et al. [24] revealed that an ideal annealing technique sharpened the phase transformation in the quaternary $Ni_{2-x}Co_xMn_{2-y}Ti_y$ series, while the Co content governs the transition's sensitivity to the external magnetic field. The direct MCE is particularly strong in the $Ni_{1.40}Co_{0.60}Mn_{1.48}Ti_{0.25}$ Heusler alloy (ΔT = 4.0 K and ΔS_{iso} = −20.0 $Jkg^{-1}K^{-1}$ under an applied magnetic field of 20 kOe). Li and coworkers [25] made a significant addition to the field by investigating the $Ni_{1.4}Co_{0.6-x}Fe_xMn_{1.4}Ti_{0.6}$ series experimentally. The partial replacement of Fe atoms with Co atoms decreases the *d*–*d* hybridizations, in this case, changing the Curie temperature and MT temperatures of the system. The maximum direct MCE value (ΔS_{iso} = −20.0 $Jkg^{-1}K^{-1}$ under a field of 50 kOe) was found for the x = 0.024 composition. By applying hydrostatic pressure (0.35 GPa), the functional response is improved, achieving values of ΔS_{iso} = −24.20 $Jkg^{-1}K^{-1}$ and RC = 347.26 JK^{-1} (under a field of 50kOe) [19]. Because this system has both direct and inverse MCE, both demagnetization and magnetization processes may be investigated for solid-state refrigeration.

It should be remarked that these materials are also under study for applications such as catalysis with chemically diverse surface configurations [26]. These materials can also have high magnetoresistance [27] and spintronic properties [28].

Researchers advocate focusing future research on the atomic site occupancy rules of these kinds of alloys. First principles and density functional theory (DFT) studies will be useful in understanding atomic site influence on the total magnetic moment per formula unit [24][25][26][27][28][29]. It is known that a large reversible magnetocaloric effect and high magnetoresistance were achieved by improving the crystallographic compatibility between the austenitic and martensitic phases [30]. Likewise, the influence of *d*–*d* hybridizations on atomic ordering may be shown by evaluating structural and magnetic properties when the quantity of the *p*-atom group decreases. Furthermore, the impact of thermal annealing, applied pressure as well as several synthesis methods on the creation of the $L2_1$ phase should be further investigated. Finally, because of the increased mechanical ductility and high induced strain values observed, the shape memory impact of ternary $Ni_{2x}Mn_{1+x}Ti_x$and $Mn_{2x}Ni_{1+x}Ti_x$ series should be further investigated.

References

1. Wei, Z.Y.; Liu, E.K.; Li, Y.; Han, X.L.; Du, Z.W.; Luo, H.Z.; Liu, G.D.; Xi, X.K.; Zhang, H.W.; Wang, W.H.; et al. Magnetostructural martensitic transformations with large volume changes and magnetostrains in all-d-metal Heusler alloys. Appl. Phys. Lett. 2016, 109, 071904.
2. Murakami, Y.; Watanabe, Y.; Kachi, S. An X-ray Study of the Heusler-type Ordering in AuAgZn2 Alloy. Trans. Jpn. Inst. Met. 1980, 21, 708–713.

3. Muldawer, L. X-ray study of ternary ordering of the noble metals in AgAuZn2 and CuAuZn2. J. Appl. Phys. 1966, 37, 2062–2066.
4. Wei, Z.Y.; Liu, E.K.; Chen, J.H.; Li, Y.; Liu, G.D.; Luo, H.Z.; Xi, X.K.; Zhang, H.W.; Wang, W.H.; Wu, G.H. Realization of multifunctional shape memory ferromagnets in all-d-metal Heusler phases. Appl. Phys. Lett. 2015, 107, 022406.
5. Ma, L.; Zhang, H.W.; Yu, S.Y.; Zhu, Z.Y.; Chen, J.L.; Wu, G.H.; Liu, H.Y.; Qu, J.P.; Li, Y.X. Magnetic-field-induced martensitic transformation in MnNiGa:Co alloys. Appl. Phys. Lett. 2008, 92, 032509.
6. Kainuma, R.; Imano, Y.; Ito, W.; Morito, H.; Sutou, Y.; Oikawa, K.; Fujita, A.; Ishida, K.; Okamoto, S.; Kitakami, O.; et al. Metamagnetic shape memory effect in a Heusler-type Ni43Co7Mn39Sn11 polycrystalline alloy. Appl. Phys. Lett. 2006, 88, 192513.
7. Zeng, Q.; Shen, J.; Zhang, H.; Chen, J.; Ding, B.; Xi, X.; Liu, E.; Wang, W.; Wu, G. Electronic behaviors during martensitic transformations in all-d-metal Heusler alloys. J. Phys. Condens. Matter. 2019, 31, 425401.
8. Feng, L. Investigation on martensitic transformation and magnetic properties of all-d-metal Pd2MnTi and Pt2MnTi by first-principle calculations. J. Supercond. Novel Magn. 2020, 33, 2245–2250.
9. Han, Y.; Wu, M.; Feng, Y.; Cheng, Z.; Lin, T.; Yang, T.; Wang, X. Competition between cubic and tetragonal phases in all-d-metal Heusler alloys, X2−xMn1+xV (X = Pd, Ni, Pt, Ag, Au, Ir, Co; x = 1, 0): A new potential direction of the Heusler family. IUCrJ 2019, 6, 465–472.
10. Han, Y.; Wu, M.; Kuang, M.; Yang, T.; Chen, X.; Wang, X. All-d-metal equiatomic quaternary Heusler hypothetical alloys ZnCdTMn (T =Fe, Ru, Os, Rh, Ir, Ni, Pd, Pt): A first-principle investigation of electronic structures, magnetism, and possible martensitic transformations. Results Phys. 2018, 11, 1134–1141.
11. Han, Y.; Bouhemadou, A.; Khenata, R.; Cheng, Z.; Yang, T.; Wang, X. Prediction of possible martensitic transformations in all-d-metal Zinc-based Heusler alloys from first-principles. J. Magn. Magn. Mater. 2019, 471, 49–55.
12. Wang, X.; Wu, M.; Yang, T.; Khenata, R. Effect of Zn doping on phase transition and electronic structures of Heusler-type Pd2Cr-based alloys: From normal to all-d-metal Heusler. RSC Adv. 2020, 10, 17829–17835.
13. Yan, H.L.; Wang, L.D.; Liu, H.X.; Huang, X.M.; Jia, N.; Li, Z.B.; Yang, B.; Zhang, Y.D.; Esling, C.; Zhao, X.; et al. Giant elastocaloric effect and exceptional mechanical properties in an all-d-metal Ni-Mn-Ti alloy: Experimental and ab-initio studies. Mater. Des. 2019, 184, 108180.
14. Shen, Y.; Sun, W.; Wei, Z.Y.; Shen, Q.; Zhang, Y.F.; Liu, J. Orientation dependent elastocaloric effect in directionally solidified Ni-Mn-Sn alloys. Scr. Mater. 2019, 163, 14–18.
15. Wei, L.; Zhang, X.; Liu, J.; Geng, L. Orientation dependent cyclic stability of the elastocaloric effect in textured Ni-Mn-Ga alloys. AIP Adv. 2018, 8, 055312.
16. Everhart, W.; Newkirk, J. Mechanical properties of Heusler alloys. Heliyon 2019, 5, e01578.
17. Ozdemir Kart, S.; Cagin, T. Elastic properties of Ni2MnGa from first-principles calculations. J. Alloys Compd. 2010, 508, 177–183.
18. Agduk, S.; Gökoğlu, G. First-principles study of elastic and vibrational properties of Ni2MnIn magnetic shape memory alloys. Eur. Phys. J. B 2011, 79, 509–514.
19. Li, Y.; Huang, S.; Wang, W.; Liu, E.; Li, L. Ferromagnetic martensitic transformation and large magnetocaloric effect in Ni35Co15−xFexMn35Ti15 (x = 2, 4, 6, 8) alloys. J. Appl. Phys. 2020, 127, 233907.
20. Cong, D.Y.; Xiong, W.X.; Planes, A.; Ren, Y.; Mañosa, L.; Cao, P.Y.; Nie, Z.H.; Sun, X.M.; Yang, Z.; Hong, X.F.; et al. Colossal elastocaloric effect in ferroelastic Ni-Mn-Ti alloys. Phys. Rev. Lett. 2019, 122, 255703.
21. Li, Y.; Qin, L.; Huang, S.; Li, L. Enhanced magnetocaloric performances and tunable martensitic transformation in Ni35Co15Mn35−xFexTi15 all-d-metal Heusler alloys by chemical and physical pressures. Sci. China Mater. 2022, 65, 486.
22. Aznar, A.; Gràcia-Condal, A.; Planes, A.; Lloveras, P.; Barrio, M.; Tamarit, J.; Xiong, W.; Cong, D.; Popescu, C.; Mañosa, L. Giant barocaloric effect in all-d-metal Heusler shape memory alloys. Phys. Rev. Mater. 2019, 3, 044406.
23. Aznar, A.; Gràcia-Condal, A.; Planes, A.; Lloveras, P.; Barrio, M.; Tamarit, J.L.; Xiong, W.; Cong, D.; Popescu, C.; Mañosa, L. DFT investigation on the electronic, magnetic, mechanical properties and strain effects of the quaternary compound Cu2FeSnS4. Crystals 2020, 10, 509.
24. Taubel, A. Tailoring magnetocaloric effect in all-d-metal Ni-Co-Mn-Ti Heusler alloys: A combined experimental and theoretical study. Acta Mater. 2020, 201, 425.
25. Li, G.; Liu, E.; Wu, G. d-d hybridization controlled large-volume-change martensitic phase transition in Ni-Mn-Ti based all-d-metal Heusler compounds. J. Alloys Compd. 2022, 923, 166369.

26. Samanta, S.; Ghosh, S.; Chatterjee, M.K. Large magnetocaloric effect and magnetoresistance in Fe-Co doped Ni50-x(FeCo)xMn37Sn13 all-d-metal Heusler alloys. J. Alloys Compd. 2022, 910, 164929.
27. Wu, M.; Zhou, F.; Khenato, R.; Kuang, M.; Wang, X. Phase transition and electronic studies of all-d-metal Heusler-type X2nTi compounds (X = Pd, Pt, Ag, Au, Cu and Ni). Front. Chem. 2020, 8, 546947.
28. Zhang, F.; Westra, K.; Shen, Q.; Batashev, I.; Kiecana, A.; van Dijk, N. The second-order magnetic phase transition and magnetocaloric effect in all-d-metal NiCoMnTi based Heusler alloy. J. Alloys Compd. 2022, 906, 164337.
29. Jin, T.; Jung, Y. Classifying intermetallic tetragonal phase of all-d-metal Heusler alloys for catalysis applications. Top. Catal. 2022, 65, 208–214.
30. Samanta, S.; Chatterjee, S.; Ghosh, S.; Mandal, K. Large reversible magnetocaloric effect and magnetoresistance by improving crystallographic compatibility condition in Ni(Co)-Mn-Ti all-d-metal Heusler alloys. Phys. Rev. Mater. 2022, 6, 094411.
